

EVOLUTION OF COMPOSITION OF MAJOR MINERAL PHASES IN LAYERED COMPLEX OF OPHIOLITE ASSEMBLAGE: EVIDENCE FOR THE VOYKAR OPHIOLITES (POLAR URALS, RUSSIA)

Evgenii V. Sharkov*, Alexei V. Chistyakov*, Evgenii E. Laz'ko* and James E. Quick**

* *Institute of Ore Deposits Geology, Petrology, Mineralogy and Geochemistry (IGEM), RAS, Moscow, Russia (e-mail: sharkov@igem.ru).*

** *U.S. Geological Survey, Mail Stop 926A, Reston, VA 20192, USA (e-mail: jquick@usgs.gov).*

Keywords: *Voykar ophiolite, layered complex, megarhythm, magmatic evolution, mineral compositions. Urals, Russia.*

ABSTRACT

We present a detailed study of compositional variation of major minerals through a cross section of the layered complex of the Late Devonian Voykar ophiolite assemblage (Polar Urals). The principal characteristics of this layered complex suggest crystallization from a periodically replenished open magma system in a tectonically dynamic, oceanic environment. The complex may be described in terms of two sequences of cumulus rocks, or megarhythms, that each display an upward progression from ultramafic to gabbroic composition. A transitional zone between the megarhythms is characterized by an upwardly reverse lithologic progression from gabbroic to ultramafic composition. Broad cryptic variation in mineral composition over intervals >100 m parallel changes in the lithologic abundances and suggest changes in the rate of magma supply relative to crystallization and/or tapping of different mantle sources that had been previously depleted to different degrees. The mineralogy, mineral compositions and isotopic composition of the layered complex coupled with the association of the Voykar ophiolite with island-arc complexes suggest that it most likely formed in a back-arc basin.

INTRODUCTION

Most recent studies suggest that layered complexes of ophiolites formed beneath small, shallow magma chambers where mantle-derived melts were stored and crystallized at spreading centers of oceans or back-arc basins (Laz'ko, 1988; Nicolas et al., 1988; Detrick, 1991; Sinton and Detrick, 1992; Quick and Denlinger, 1992, 1993). The appearance and distribution of lithologies in these complexes are reminiscent of continental layered intrusions (Laz'ko and Sharkov, 1988; Sharkov and Smolkin, 1998), which suggests that similar magmatic processes may be at work in the oceanic and continental crusts. Detailed studies of rock successions and mineral compositions through cross sections of oceanic and continental layered complexes help to develop and test models for the processes involved in the evolution of these important magmatic systems. In this paper, we report mineral chemistry for a detailed transect across the layered complex of one of the best preserved Voykar ophiolite sections, Polar Urals, Russia.

GEOLOGICAL SETTING

The Ural Mountains expose a narrow belt of Palaeozoic rocks between the European continent and the North-Asian (East-Uralian, or Kazakhstan) continent to the east (Fig. 1). During the Late Permian collision of these continents, the Ural ocean was closed and large tectonic sheets of pelagic sediments, oceanic lithosphere and island-arc rocks were transported westward over shelf deposits of the passive margin of the Russian craton (Zonenshain et al., 1990; Puchkov, 1997; Ivanov, 1998). Tectonic fragments of oceanic lithosphere and island-arc complexes are now exposed along the eastern slope of the Urals, comprising several ophiolite belts within a zone about 2000 km in length and to 250 km in width.

The Main Uralian fault zone, the major tectonic element of the region, is a zone of shearing and serpentinite mélangé about 20 km wide that extends along the entire length of the mountain ridge. Transport of oceanic and island-arc rocks occurred along this structure and onto the continental margin. Well-preserved ophiolite massifs in the vicinity of the Main Uralian fault zone are nappes or giant blocks within serpentinite mélangé. One of them is the Voykar-Syn'nsky massif in the Polar Urals, which is about 200 km long and 20 km wide and consists of southwest-dipping thrust sheets (Fig. 1; Saveliev and Savelieva, 1977; Efimov et al., 1978; Savelieva, 1987; Laz'ko, 1988; Saveliev, 1997). Taken together the thrust sheets form a typical ophiolite association. The lowest, which is named the Khulga sheet, contains up to 4 km intensely deformed and metamorphosed gabbro. Above it is the 1- to 9-km-thick Payer sheet, which contains mantle peridotites, lower-crustal ultramafic and gabbroic rocks, and diabases of a sheeted dike complex. The overlying Lagorta sheet is about 1.5 km in thickness and consists mainly of quartz diorite and tonalite that display intrusive contacts with sheeted dikes and gabbro of the Voykar ophiolite.

Mantle ultramafic rocks are the deepest rocks in the section of the Payer sheet. They consist mainly of spinel harzburgite cut by sparse, irregular veins of dunite, websterite, and bronzitite. The mantle ultramafic rocks are overlain by a >3500-m-thick layered complex consisting of interlayered ultramafic to gabbroic rocks.

At the base of the layered complex and overlying the mantle harzburgite is a >1000-m-thick sequence of dunite containing layers of pyroxenite and gabbro, herein referred to as the marginal dunite. The transition between well layered rocks and the marginal dunite is gradational with pyroxenite and gabbro layers decreasing in abundance downward. Based on this relationship, the senior authors of this study have chosen to assign the marginal dunite to the layered complex. The transition between the mantle harzburgite

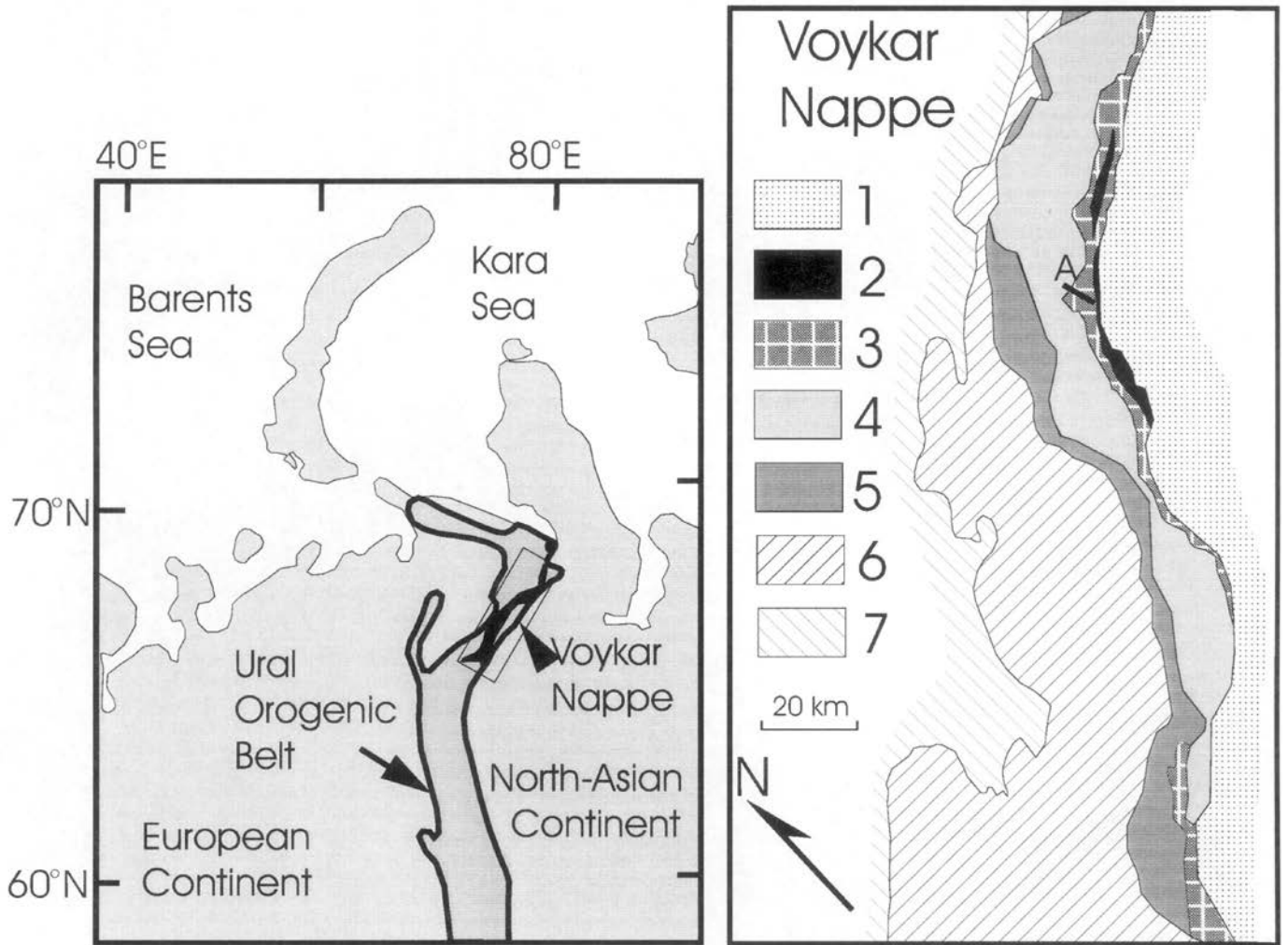


Fig. 1 - Schematic map of the Voykar massif after Sharma et al. (1995). 1- dioritic and tonalitic rocks of the Lagorta thrust sheet and arc volcanics; 2-4- Voykar ophiolites: 2- sheeted dikes, 3- gabbro and cumulate ultramafic rocks; 4 - mantle peridotites; 5- metamorphosed gabbro, plagiogranite and marble of the Khulga thrust sheet; 6- pelagic and volcanic-sedimentary rocks; 7- shelf deposits. A - location of the cross section.

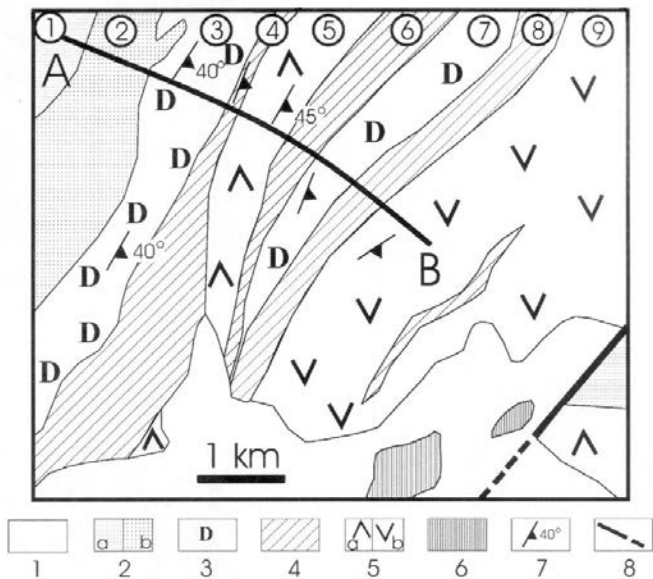


Fig. 2 - Schematic map of the studied area, modified after Efimov et al. (1978). 1- Quaternary deposits; 2- mantle harzburgite: a- slightly altered, b- strongly altered; 3- dunite; 4- horizons of alternation of basic and ultrabasic rocks; 5- gabbroic rocks: a- gabbro, b- gabbro-norite; 6- diabase of the sheeted dike complex; 7- bedding; 8- tectonic boundary of nappes. A-B- location of the cross-section.

gite and the marginal dunite is also gradational through a zone of lens-like alternations of tectonized harzburgite and dunite with dunite decreasing and harzburgite increasing downward in the section. These relationships are similar to those in the Oman ophiolite where a thick dunite “transition zone” is present between mantle harzburgite and layered gabbro (Nicolas et al., 1988). Most investigators would assign the dunite “transition zone” in Oman to the mantle section, thus placing it beneath the Moho. Although not adopted here, a similar assignment in the Voykar ophiolite would place the Moho and the base of the layered complex at the base of the wehrlite unit corresponding to sample 370 in Fig. 4.

The petrology and geochemistry of the mantle peridotite has been well characterized (Savelieva, 1987; Laz'ko, 1988; Sharma et al., 1995, etc.), but there is little published data on the petrology and structure of the layered complex. Because of this, E.E. Laz'ko carried out a detailed sampling through the complex along the Truba-Yu River in the northern part of the Voykar massif. A schematic map of this area and a geological section are represented in Figs. 2 and 3, and a representative columnar section is shown in Fig. 4.

Along the studied section, rocks of the layered complex dip monoclinaly eastward at 20° to 70° with an average dip of 40-50° (Figs. 2 and 3). Local irregularities in dip and the

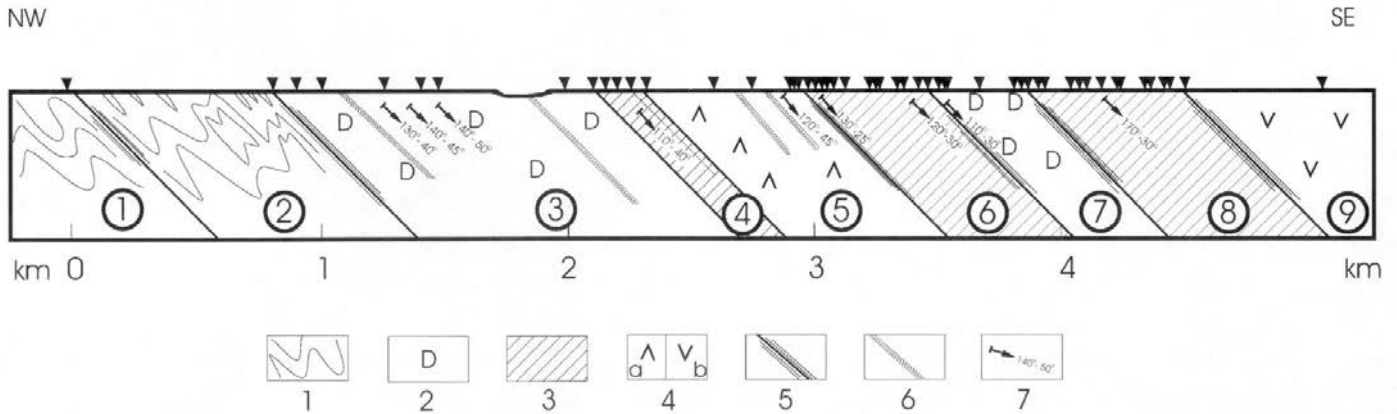


Fig. 3 - Geological cross-section of the Layered complex. 1- mantle harzburgite; 2- dunite; 3- horizons of alternation of basic and ultrabasic rocks; 4- gabbroic rocks: a- gabbro, b- gabbro-norite; 5- boundaries between units; 6- thrusts; 7- bedding. Black triangles- sample locations. *Numbers in circles*: 1-2- mantle harzburgite: 1- mildly altered, 2- strongly altered; 3-5- the lower megarhythm: 3- marginal dunite, 4- horizon of alternation, 5- gabbro; 6- the transitional zone; 7-9- the upper megarhythm: 7- dunite, 8- horizon of alternation, 9- gabbro-norite.

occurrence of similar rock types at various places in the section have been taken as evidence of repetition by isoclinal folding (Efimov et al., 1978). However, our investigation found that potentially repeated units are in fact distinct in internal structure and composition. We conclude that the exposed section approximates a relatively simple "stratigraphic succession" that has been tilted but not repeated by isoclinal folding, although some tectonic discontinuities cannot be ruled out.

Stratigraphically, the section may be described in terms of two sequences of cumulus rocks, or megarhythms, that range in composition upward from ultramafic to gabbroic (Fig. 4). The lower megarhythm begins with the marginal dunite, which contains sparse, thin layers of wehrlite. This unit grades into a 130-m-thick sequence of interlayered dunite, wehrlite, olivine clinopyroxenite and clinopyroxenite within which dunite is the dominant lithology. Overlying this are 600 m of layered gabbro and massive gabbro with sparse layers of clinopyroxenite at the highest stratigraphic levels. Above the lower megarhythm is a 500-m-thick sequence of interlayered dunite and wehrlite referred to herein as the transitional zone.

The upper megarhythm overlies the transition zone and begins with 300-m-thick zone of dunite. In the lower part of this unit, veins of olivine gabbro-norite occur. Above this unit are 600 m of interlayered wehrlite, clinopyroxenite, gabbro and olivine gabbro, olivine gabbro-norite and gabbro-norite. In most of this part of the section, rhythmic layering occurs and the rocks are strongly sheared. A thick 300-m-thick zone of gabbro-norite and olivine gabbro-norite completes the studied section; a thin layer of dunite occurs at the base of this unit.

The best age constraint on the formation of the Voykar ophiolite is provided by a Sm-Nd isotopic study by Sharma et al. (1995), which yielded an age of 387 ± 34 Ma and an initial ϵNd of 8.6 ± 1.8 . This study also determined that the oceanic crustal rocks and most (but not all) of the mantle harzburgite samples had isotopic compositions consistent with a melt-residuum relationship involving the same MORB source, and that the major-element and low-REE-composition of the Voykar harzburgite can be modeled by progressive extraction of melt from an undepleted mantle protolith with the requirement that melt separation began in the garnet lherzolite stability field.

ANALYTICAL TECHNIQUES

Samples of rocks displaying minimal alteration were systematically collected every 50 to 100 m in the section. More detailed sampling (about 90 samples) was performed in parts of the section that had thin layering.

Major and minor element analyses were obtained with a JEOL 8900 electron microprobe at the US Geological Survey in Denver, Colorado. Analyses were corrected using on-line ZAF oxide correction procedures. Replicate analyses of secondary standards indicate a relative analytical precision of better than $\pm 1\%$ (1 sigma) for major elements and precision equal to counting statistics for minor elements. About 1200 mineral analyses were performed using conditions of 15 kV accelerating voltage and 20 nA sample current on brass. Representative analyses are presented in Tables 1 through 7. All analyses are presented graphically in Figs. 5-8.

PETROGRAPHY AND MINERALOGY OF ROCKS

Unlike most continental layered intrusions, which consist of relatively undeformed magmatic rocks, virtually all rocks of the Voykar layered complex are blastomylonites that were deformed at high temperature. Cumulate textures in these rocks are only locally preserved and, strictly speaking, the rocks are metamorphosed plutonic rocks. Nevertheless, we have chosen to refer to them using igneous rather than metamorphic names to emphasize the primary lithologic variations, which are igneous in origin.

In addition to high-temperature recrystallization, ultramafic rocks have been extensively serpentinized and pyroxene and plagioclase in gabbroic rocks have been replaced by actinolite and saussurite, respectively. Near the overlying layered complex, the mantle peridotite is strongly altered and transformed into amphibole- and antigorite-olivine schist.

Mantle Peridotites

Mantle peridotite in the Voykar ophiolite consists of mainly harzburgite with protogranular to porphyroclastic textures (Nicolas, 1989). The principal phases have the following volume proportions: 65-80% olivine (Fo^{90-91}); 20-

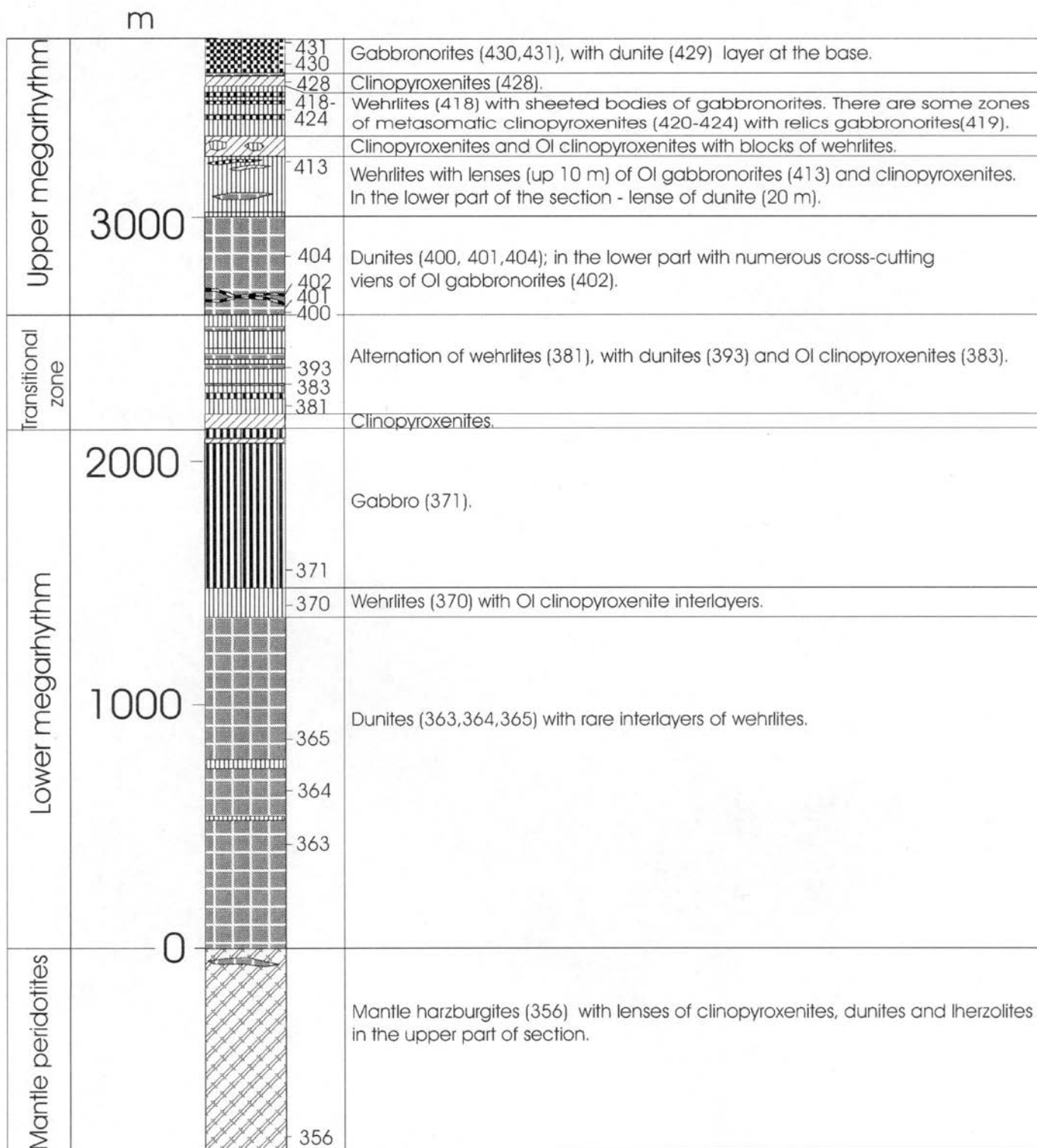


Fig. 4 - Stratigraphic cross section of the Layered complex of the Voykar ophiolite assemblage showing sample number and location of the samples for which data are reported in Tables 1-7.

30% orthopyroxene ($Wo^{1}En^{90}Fs^{9}$); 1-7% clinopyroxene ($Wo^{50-51}En^{45-47}Fs^{3-4}$); <1-2% chromian spinel; and ≤ 1 % pale-green hornblende.

Protogranular rocks are coarse-grained intergrowths of olivine and orthopyroxene with small amounts of interstitial clinopyroxene and hornblende. Large grains of olivine and orthopyroxene are subidiomorphic to xenomorphic; smaller grains are hypidiomorphic or rounded. Large grains of olivine and orthopyroxene with wavy extinction and defor-

mation twinning are abundant. Clinopyroxene exsolution lamellae are present in cores of large orthopyroxene grains; small orthopyroxene grains (0.1-0.2 mm) are usually free of lamellae. They are commonly accompanied by hornblende, sometimes in evident replacement relationship. Translucent red-brown chromian spinel occurs as subidiomorphic or curved "wormy" grains; $Cr^{2}O^{3}$ content in one of studied sample is 23.0-25.6 wt.%, and $Al^{2}O^{3}$ - 41.7-43.3 wt.%.

In porphyroclastic rocks, olivine and orthopyroxene form

Table 1 - Representative analyses of olivine from the Voykar ophiolite assemblage (wt.%)

Sample	356	363	364	393	400	404	405	429	381	383	418	423	402	413
SiO ₂	41.17	40.58	41.61	40.60	40.87	41.21	40.86	40.75	38.93	40.58	40.52	40.46	39.64	38.50
FeO	8.60	11.17	10.41	12.24	9.39	8.42	10.87	10.33	17.05	16.08	15.27	16.35	19.83	25.6
MnO	0.13	0.17	0.16	0.22	0.19	0.12	0.19	0.28	0.26	0.23	0.26	0.21	0.35	0.32
MgO	49.57	47.84	48.84	46.27	48.88	50.42	48.63	47.97	43.18	44.32	44.72	44.23	40.67	36.77
CaO	0.00	0.02	0.06	0.02	0.02	0.04	0.01	0.01	0.03	0.02	0.03	0.03	0.00	0.01
NiO	0.45	0.25	0.28	0.26	0.16	0.13	0.24	0.26	0.06	0.09	0.13	0.14	0.07	0.10
Total	99.92	100.03	101.39	99.67	99.55	100.38	100.84	99.61	99.54	101.34	100.97	101.45	100.60	101.33
Fo	0.91	0.88	0.89	0.87	0.90	0.91	0.89	0.89	0.82	0.83	0.84	0.83	0.79	0.72

Notes (here and follows): Mantle complex: 356 - harzburgite. Layered complex: the lower megarhythm: 363-365 -dunites, 370 - wehrlite, 371-gabbro; the transitional zone: 381 - wehrlite, 383 - Ol clinopyroxenite, 393 - dunite; the upper megarhythm: 400,401,404 and 429 - dunite, 402 and 423 - Ol gabbro-norites, 418 and 424 - wehrlite, 419,430 and 431 - gabbro-norites, 420-421 - metasomatic clinopyroxenites, 423 - Ol clinopyroxenite and 428 - clinopyroxenite.

Table 2 - Representative analyses of clinopyroxene from the Voykar ophiolite assemblage (wt.%)

Sample	356	363	364	370	371	381	381	383	388	388	393	402	404
SiO ₂	53.18	52.85	53.81	53.05	52.55	53.24	52.68	53.10	53.85	53.79	54.34	53.18	54.33
TiO ₂	0.14	0.29	0.29	0.15	0.24	0.07	0.13	0.09	0.12	0.08	0.09	0.18	0.06
Al ₂ O ₃	2.89	2.49	2.50	2.59	2.78	2.15	2.83	2.95	2.46	2.84	1.23	2.53	1.40
Cr ₂ O ₃	0.70	0.52	0.68	0.69	0.12	0.16	0.36	0.70	0.53	0.66	0.31	0.12	0.68
FeO	1.77	2.84	2.48	3.28	5.38	4.08	4.43	3.96	3.93	4.54	2.48	4.51	1.83
MnO	0.08	0.09	0.10	0.12	0.18	0.14	0.14	0.15	0.12	0.10	0.09	0.17	0.09
MgO	16.53	16.33	16.73	16.41	15.66	15.88	16.34	15.93	16.09	17.21	16.61	15.72	17.18
CaO	24.27	23.87	23.76	23.90	22.61	23.91	22.62	23.81	23.44	21.74	24.42	23.30	24.16
Na ₂ O	0.16	0.21	0.30	0.22	0.24	0.04	0.10	0.09	0.13	0.11	0.10	0.16	0.27
K ₂ O	0.02	0.02	0.02	0.02	0.03	0.02	0.01	0.00	0.02	0.03	0.01	0.02	0.03
NiO	0.07	0.05	0.04	0.02	0.01	0.07	0.07	0.01	0.00	0.00	0.03	0.03	0.00
Total	99.81	99.56	100.71	100.45	99.80	99.76	99.71	100.79	100.69	101.10	99.71	99.92	100.03
En	0.47	0.47	0.47	0.46	0.45	0.45	0.47	0.45	0.46	0.49	0.47	0.45	0.48
Wo	0.50	0.49	0.49	0.49	0.47	0.49	0.46	0.49	0.48	0.44	0.49	0.48	0.49
Fs	0.03	0.05	0.04	0.05	0.09	0.06	0.07	0.06	0.06	0.07	0.04	0.07	0.03

Sample	413	413	418	419	420	421	423	424	424	424	428a	430	431
SiO ₂	51.21	51.98	52.86	53.19	52.45	53.37	53.40	54.19	57.70	53.18	54.85	52.29	51.70
TiO ₂	0.31	0.26	0.17	0.08	0.14	0.14	0.09	0.07	0.03	0.16	0.00	0.35	0.30
Al ₂ O ₃	3.52	3.33	3.20	2.33	2.67	2.92	2.67	1.65	2.06	3.27	0.08	2.57	2.76
Cr ₂ O ₃	0.01	0.02	0.71	0.35	0.25	0.40	0.50	0.31	0.28	0.57	0.21	0.02	0.00
FeO	7.13	8.99	4.09	4.68	4.70	4.60	4.09	3.74	2.66	5.32	3.16	9.16	7.05
MnO	0.15	0.21	0.10	0.11	0.14	0.12	0.13	0.10	0.10	0.11	0.11	0.27	0.20
MgO	14.26	15.10	15.99	16.21	16.09	15.87	15.97	16.62	22.79	17.85	16.45	12.91	14.32
CaO	23.31	20.2	22.96	23.12	23.3	23.3	23.55	24.25	12.80	20.13	25.17	22.52	22.84
Na ₂ O	0.18	0.20	0.16	0.17	0.15	0.12	0.13	0.05	0.47	0.12	0.04	0.22	0.23
K ₂ O	0.02	0.03	0.02	0.03	0.02	0.03	0.01	0.02	0.04	0.03	0.02	0.00	0.02
NiO	0.00	0.02	0.01	0.02	0.03	0.00	0.04	0.00	0.00	0.05	0.05	0.00	0.05
Total	100.10	100.30	100.27	100.29	99.94	100.87	100.58	101.00	98.93	100.79	100.14	100.31	99.47
En	0.41	0.44	0.46	0.46	0.45	0.45	0.45	0.46	0.68	0.51	0.45	0.38	0.41
Wo	0.48	0.42	0.47	0.47	0.47	0.48	0.48	0.48	0.28	0.41	0.50	0.47	0.47
Fs	0.11	0.15	0.07	0.07	0.07	0.07	0.07	0.06	0.04	0.08	0.05	0.15	0.11

Table 3 - Representative analyses of orthopyroxene from the Voykar ophiolite assemblage (wt.%)

Sample	356	383	388	391	402	403	406	409	412	413	418	419	420	421	423	427	433
SiO ₂	55.98	55.2	55.4	55.33	55.41	54.72	56.3	55.69	56.32	54.18	55.72	55.2	55.53	55.52	55.98	54.87	54.85
TiO ₂	0.04	0.06	0.04	0.03	0.07	0.08	0.03	0.10	0.03	0.06	0.07	0.05	0.00	0.02	0.03	0.05	0.04
Al ₂ O ₃	3.34	2.87	3.29	2.45	1.96	2.24	1.08	2.05	1.57	2.14	2.45	1.87	1.92	2.44	2.48	2.22	2.34
Cr ₂ O ₃	0.59	0.42	0.49	0.37	0.04	0.04	0.36	0.42	0.33	0.01	0.44	0.22	0.16	0.40	0.33	0.33	0.30
FeO	5.96	10.84	10.89	10.53	12.05	13.42	10.15	10.99	9.23	16.93	9.89	12.06	11.72	12.00	10.91	10.97	12.05
MnO	0.12	0.23	0.24	0.25	0.32	0.33	0.29	0.26	0.21	0.33	0.24	0.26	0.31	0.32	0.23	0.22	0.32
MgO	33.76	30.29	29.98	30.91	29.54	28.27	31.07	30.07	31.52	26.18	30.68	29.65	30.01	29.44	30.46	30.39	29.25
CaO	0.60	0.87	0.61	0.48	0.73	0.78	0.79	0.76	0.69	0.74	0.66	0.67	0.58	0.63	0.61	0.64	0.78
NiO	0.07	0.01	0.07	0.00	0.01	0.01	0.05	0.06	0.06	0.00	0.06	0.04	0.02	0.00	0.02	0.06	0.00
Total	100.46	100.79	101.01	100.35	100.13	99.89	100.12	100.40	99.96	100.57	100.21	100.02	100.25	100.77	101.05	99.75	99.93
En	0.90	0.82	0.82	0.83	0.80	0.78	0.83	0.82	0.85	0.72	0.84	0.80	0.81	0.80	0.82	0.82	0.80
Wo	0.01	0.02	0.01	0.01	0.01	0.02	0.02	0.01	0.01	0.01	0.01	0.01	0.01	0.01	0.01	0.01	0.02
Fs	0.09	0.16	0.17	0.16	0.18	0.21	0.15	0.17	0.14	0.26	0.15	0.18	0.18	0.18	0.17	0.17	0.18

Table 4 - Representative analyses of plagioclase from the Voykar ophiolite assemblage (wt.%)

Sample	384	403	413	413	419	419	420	420	427	427	427	430	430
SiO ₂	44.78	44.58	44.5	44.94	44.97	44.56	44.47	44.51	44.84	42.91	44.51	46.23	45.98
Al ₂ O ₃	35.44	35.12	35.57	35.10	34.69	35.44	35.06	35.58	35.26	35.81	35.12	33.97	34.45
FeO	0.19	0.19	0.20	0.48	0.20	0.16	0.23	0.08	0.23	0.27	0.25	0.10	0.26
CaO	19.03	19.28	19.36	18.98	18.40	19.16	19.45	19.55	19.69	20.26	19.64	18.07	18.19
Na ₂ O	0.59	0.58	0.48	0.76	0.87	0.43	0.44	0.34	0.35	0.18	0.31	1.20	1.11
K ₂ O	0.02	0.03	0.02	0.02	0.03	0.03	0.02	0.02	0.02	0.01	0.03	0.02	0.03
Total	100.05	99.78	100.13	100.28	99.16	99.78	99.67	100.08	100.39	99.44	99.86	99.59	100.02
An	0.95	0.95	0.96	0.93	0.92	0.96	0.96	0.97	0.97	0.98	0.97	0.89	0.9

Table 5 - Representative analyses of amphiboles from the Voykar ophiolite assemblage (wt.%)

Sample	356	371	386	393	402	413	418	419	419	420	423	427	428a	431a
SiO ₂	50.79	45.72	51.61	52.81	46.15	46.20	46.86	48.46	49.14	46.78	47.42	49.16	51.93	45.46
TiO ₂	0.12	0.18	0.15	0.07	0.33	0.41	0.36	0.34	0.30	0.36	0.45	0.00	0.09	0.44
Al ₂ O ₃	2.89	12.32	2.23	2.03	11.99	12.08	11.04	9.25	9.25	10.97	11.08	10.06	2.76	11.39
Cr ₂ O ₃	0.60	0.11	0.61	0.82	0.12	0.00	0.96	0.34	0.81	0.29	1.34	0.01	0.26	0.06
FeO	3.33	7.47	3.28	2.60	7.70	8.96	5.96	6.84	6.61	7.27	6.44	6.24	4.01	10.81
MnO	0.09	0.14	0.12	0.13	0.13	0.09	0.06	0.08	0.07	0.05	0.04	0.09	0.11	0.18
MgO	16.21	15.59	16.33	16.64	16.84	15.69	17.48	17.68	17.75	17.39	17.05	17.83	16.47	13.71
CaO	22.86	12.54	24.02	23.13	12.08	12.18	12.57	12.18	12.19	12.35	12.38	12.84	22.72	11.99
Na ₂ O	0.16	2.45	0.08	0.19	1.86	1.98	1.57	1.86	1.77	1.82	1.82	0.97	0.08	1.46
K ₂ O	0.02	0.14	0.01	0.03	0.14	0.15	0.09	0.04	0.03	0.09	0.03	0.02	0.04	0.05
NiO	0.03	0.04	0.04	0.02	0.00	0.02	0.03	0.05	0.06	0.05	0.04	0.02	0.00	0.03
Total	97.10	96.69	98.47	98.46	97.34	97.75	96.98	97.12	97.97	97.44	98.07	97.23	98.47	95.57

Table 6 - Representative analyses of chromespinel from the Voykar ophiolite assemblage (wt.%)

Sample	356	363	364	370	383	388	393	400	404	405	418	423	424	427	429
TiO ₂	0.07	0.52	0.42	0.16	0.12	0.15	0.16	0.26	0.19	0.21	0.24	0.33	0.30	0.26	0.17
Al ₂ O ₃	41.82	26.21	27.48	33.94	28.36	32.95	23.89	18.52	17.44	9.85	29.49	24.31	30.10	24.96	28.93
Cr ₂ O ₃	25.6	31.15	34.73	28.13	24.63	25.29	35.88	41.92	45.24	52.56	25.43	26.87	23.12	25.18	27.9
Fe ₂ O ₃	2.90	11.03	6.53	6.94	14.71	9.36	7.33	7.21	7.32	7.41	12.67	16.28	14.09	17.46	10.6
FeO	11.89	20.61	17.74	19.76	25.84	21.39	22.38	22.51	16.09	23.44	23.98	23.44	24.77	23.52	19.34
MnO	0.21	0.33	0.33	0.32	0.41	0.43	0.41	0.48	0.38	0.57	0.35	0.34	0.38	0.34	0.65
MgO	17.20	10.10	11.94	11.50	6.83	9.97	8.16	7.62	11.63	6.43	8.11	7.71	7.72	7.72	10.39
NiO	0.24	0.15	0.12	0.04	0.08	0.08	0.04	0.00	0.08	0.02	0.14	0.14	0.11	0.16	0.16
Total	99.93	100.10	99.29	100.79	101.00	99.63	98.25	98.52	98.39	100.49	100.42	99.49	100.59	99.63	98.15
Cations on 4 oxygen basic															
Al	1.37	0.96	0.99	1.18	1.04	1.17	0.9	0.72	0.66	0.39	1.07	0.91	1.09	0.94	1.06
Cr	0.56	0.76	0.84	0.66	0.61	0.60	0.91	1.09	1.15	1.41	0.62	0.68	0.56	0.63	0.68
Fe ³	0.06	0.26	0.15	0.15	0.34	0.21	0.18	0.18	0.18	0.19	0.29	0.39	0.33	0.42	0.25
Fe ²	0.28	0.53	0.45	0.49	0.67	0.54	0.6	0.62	0.43	0.66	0.62	0.63	0.64	0.63	0.5
Mg	0.71	0.47	0.54	0.51	0.32	0.45	0.39	0.37	0.56	0.32	0.37	0.37	0.36	0.37	0.48

Table 7 - Representative analyses of magnetite from the Voykar ophiolite assemblage (wt.%)

Sample	413	413	413	413	424	428a
TiO ₂	0.53	6.21	1.15	5.15	0.72	0.68
Al ₂ O ₃	1.03	1.37	1.26	1.24	0.27	0.04
Cr ₂ O ₃	0.19	0.20	0.16	0.22	8.68	0.00
Fe ₂ O ₃	66.19	55.5	65.93	58.02	59.1	67.57
FeO	31.24	36.54	32.28	35.60	30.82	31.15
MnO	0.03	0.23	0.05	0.19	0.16	0.06
MgO	0.12	0.22	0.19	0.28	0.57	0.17
NiO	0.07	0.04	0.03	0.05	0.19	0.14
Total	99.40	100.31	101.05	100.75	100.51	99.81
Cations on 4 oxygen basis						
Ti	0.02	0.18	0.03	0.15	0.02	0.02
Al	0.05	0.06	0.06	0.06	0.01	0.00
Cr	0.01	0.01	0.00	0.01	0.26	0.00
Fe ³	1.92	1.58	1.87	1.65	1.69	1.96
Fe ²	1.01	1.16	1.02	1.12	0.98	1.00
Mg	0.01	0.01	0.01	0.02	0.03	0.01

elongate, strained porphyroclasts \leq 5-6 mm in diameter. Strain is seen as moderate to strong undulatory extinction or kink-bands in olivine and curved exsolution lamellae in orthopyroxene; deformation twinning is common in porphyroclasts. The neoblast assemblage consists of olivine, orthopyroxene, clinopyroxene, spinel and interstitial pale-green hornblende in all samples. Neoblasts of olivine and orthopyroxene are present as small (\leq 1 mm) polygonal, mildly strained to strain-free grains along grain boundaries and in trails through olivine and orthopyroxene porphyroclasts.

Layered Complex

Dunite consists of a medium- to coarse-grained intergrowth of mainly olivine (Fo⁸⁸⁻⁹¹) and minor amounts (2-5 vol.%) of xenomorphic chromian spinel and diopside (Wo⁴⁸⁻⁵⁰En⁴⁶⁻⁴⁸Fs²⁻⁶). Olivine grains have rounded or complicated shapes and show optical evidence of strain. Compositions of olivine and clinopyroxene are relatively uniform in dunite throughout the section. In contrast, compositions of chromian spinel show more clearly definable variation with stratigraphic position. In the marginal dunite of the lower megarhythm, spinel is composed of 29.7 to 35.1 wt.% Cr²O₃ and 20.7-29.8 wt.% Al²O₃. The lowest Cr concentration in spinel occurs in the middle part of this horizon. In the dunite of the upper megarhythm, the Cr²O₃ content of chromian spinel increases from 40.4 to 52.8 wt.%, and Al²O₃ decreases from 20.1 to 7.9 wt.%. Spinel is more Cr-rich and contains less Al-rich when it is included in clinopyroxene and more ferrous and Al-rich when it is included in olivine.

Wehrlite and olivine clinopyroxenite differ from each other only in their olivine contents, which range from 30 to 40 vol.% in the former and 10 to 20 vol.% in the latter. Olivine sometimes has an oval shape, but a complicated morphology is more typical. Clinopyroxene porphyroclasts form large elongated strained grains with rounded edges that in some cases approach a subidiomorphic shape. Some grains of clinopyroxene contain lamellae of orthopyroxene, but, as a rule, they are replaced by small irregular grains of pale-green hornblende. The neoblast assemblage consists of small polygonal grains of clinopyroxene and olivine that are situated along grain boundaries or in trails through clinopyroxene porphyroclasts.

In wehrlite and clinopyroxenite of the transitional zone, sparse grains of orthopyroxene and spinel occur locally. As in dunite, higher Cr contents are found in spinels included in clinopyroxene and higher Al contents are found in spinels included in olivine. Locally, interstitial plagioclase (An⁹⁷⁻⁹⁸) occurs, but is extensively replaced by chlorite.

The composition of olivine and clinopyroxene in wehrlite and olivine clinopyroxenite is nearly uniform throughout the layered complex (Fo^{82-84} and $\text{Wo}^{42-50}\text{En}^{43-47}\text{Fs}^{3-7}$, respectively). The composition of orthopyroxene in the upper megarhythm is $\text{Wo}^{1-2}\text{En}^{81-85}\text{Fs}^{13-15}$. In the transitional zone, orthopyroxene is slightly more ferrous ($\text{Wo}^{1-2}\text{En}^{81-84}\text{Fs}^{16-18}$). The compositions of porphyroclastic and neoblastic forms of the same phase are practically the same.

Clinopyroxenite has two modes of occurrence in the layered complex. (1) Clinopyroxenite layers similar to those described above but without olivine are interpreted to be former cumulates. (2) Clinopyroxenite also forms vein- or lens-like bodies with teeth-like textures typical of metasomatic rocks are found in the upper megarhythm where they replace a variety of rocks ranging from pyroxenite to gabbro. The clinopyroxene compositions in the first type of occurrence are effectively the same as in the olivine clinopyroxenite. However, clinopyroxene in the second type of occurrence are subcalcium augite to pigeonite-augite in composition ($\text{Wo}^{28-29}\text{En}^{66-68}\text{Fs}^{5-6}$). Chromian spinel is absent in these clinopyroxenites and magnetite is the principal oxide phase.

Gabbro constitutes the most abundant rock type in the layered complex. Typically, gabbro is strongly affected by low-T alteration and only locally are the high-temperature textures and minerals well preserved. In these cases, cumulate textures are extremely scarce and the rock texture is dominantly granoblastic with a grain size of ≤ 1.5 mm. Relic mineral assemblages and non-altered samples suggest that lithologic variations include gabbro, olivine gabbro, gabbro, and olivine gabbro. Rocks with orthopyroxene are found only in the upper part of the studied section.

Plagioclase forms slightly elongated grains that are free of zoning and are only slightly strained. Some plagioclase grains contain small rounded inclusions of pyroxene (mainly clinopyroxene). Pyroxene grains are also slightly elongated, but the morphology of olivine grains is complex, consisting of elongated, curved, hook-like shapes. Undulatory extinction indicates that olivine is mildly strained. Pale-green hornblende (3-5 vol.%) forms oikocrysts that enclose small rounded grains of pyroxene and olivine. These hornblende oikocrysts are interpreted to be late-stage magmatic phases. They are free of deformation features, indicating that high-temperature deformation had effectively run its course in these rocks while they were still above their solidus. Magnetite forms irregular grains in the interstices of silicate minerals and forms symplectic aggregates with orthopyroxene that constitute up to 5 vol. % of the rocks.

Plagioclase from the lower megarhythm is almost totally altered. In the gabbro from the upper megarhythm, plagioclase composition ranges from An^{92-96} to An^{89-90} in the upper part of the section.

The composition of clinopyroxene in gabbroic rocks varies progressively upward from $\text{Wo}^{42-49}\text{En}^{43-47}\text{Fs}^{5-11}$ in the gabbro of the lower megarhythm to $\text{Wo}^{45-48}\text{En}^{38-47}\text{Fs}^{7-16}$ in gabbro of the upper horizon of the upper megarhythm. In olivine gabbro veins from the dunite horizon of the upper megarhythm, clinopyroxene is more magnesian ($\text{Wo}^{47-48}\text{En}^{44-45}\text{Fs}^{7-8}$) than clinopyroxene from the overlying gabbro ($\text{Wo}^{42-48}\text{En}^{41-46}\text{Fs}^{10-15}$).

Orthopyroxene is absent in gabbroic rocks of the lower megarhythm. In gabbro of the upper megarhythm, its composition is $\text{Wo}^{1-2}\text{En}^{69-74}\text{Fs}^{25-30}$. In olivine gabbro veins, it is more magnesian ($\text{Wo}^{1-2}\text{En}^{80-81}\text{Fs}^{18-19}$).

The composition of olivine in gabbroic rocks is Fo^{79-81} ,

and only in some lenses of gabbro in the upper layered horizon it is more ferrous (Fo^{71-73}). Fine double-rim textures sometimes are found along the boundaries of olivine and plagioclase.

COMPOSITIONAL VARIATION OF MAJOR MINERALS

Figs. 5 and 6 illustrate that cryptic variation in $\text{Mg}/(\text{Mg}+\text{Fe})$ occurs at two scales in the Voykar layered complex. Best defined are broad Fe-enrichment and -depletion trends on the scale of 500 to 1000 m. Within these broad trends are clear indications of a "higher frequency" signal consisting of smaller reversals on the scale of <100 m. The stratigraphic sampling interval used for most of this study, 50 to 100 m, was probably too coarse to more completely describe the higher frequency variations.

Careful analysis of the data reveals that the $\text{Mg}/(\text{Mg}+\text{Fe})$ variation of the dominant mafic silicates, olivine and clinopyroxene, correlate with the lithology of the host rock (Figs. 5 and 6B). Forsterite content of olivine is Fo^{88-91} in dunite, Fo^{82-84} in wehrlite and olivine clinopyroxenite, Fo^{79-81} in gabbro, and Fo^{71-73} in gabbro. Similarly, the composition of clinopyroxene ranges from $\text{Wo}^{48-50}\text{En}^{46-48}\text{Fs}^2$ in dunite, $\text{Wo}^{42-50}\text{En}^{43-47}\text{Fs}^{3-7}$ in wehrlite and clinopyroxenite, $\text{Wo}^{42-49}\text{En}^{43-47}\text{Fs}^{5-11}$ in gabbro, and $\text{Wo}^{45-48}\text{En}^{38-47}\text{Fs}^{7-16}$ in gabbro. The compositional ranges of these lithologies

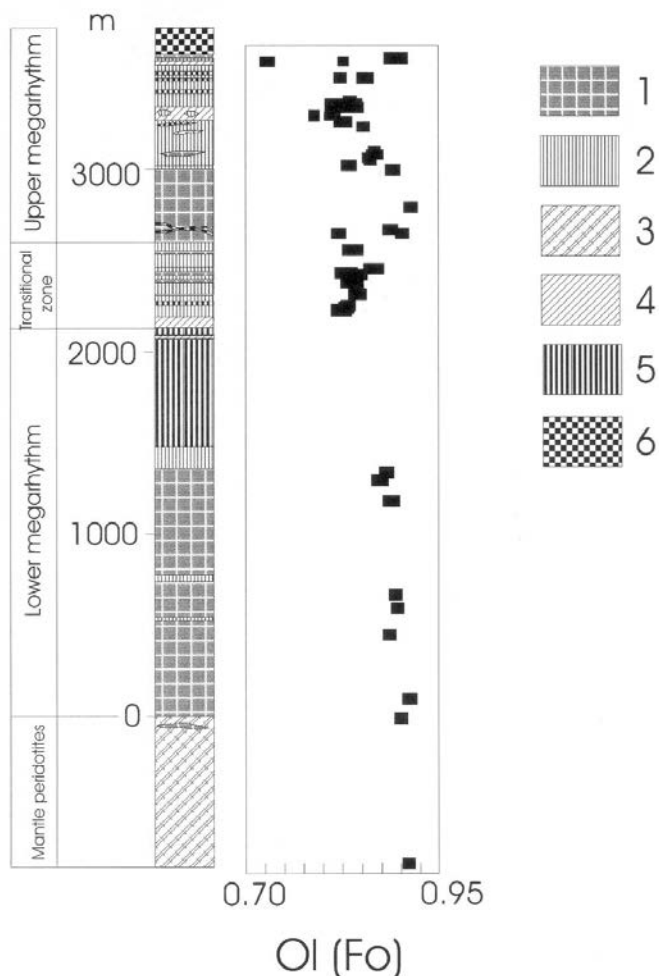


Fig. 5 - Forsterite content of olivine through the section. Ornamentation: 1- dunite; 2- wehrlite; 3- harzburgite; 4- clinopyroxenite; 5- gabbro and gabbro; 6- the uppermost gabbro.

remain distinct regardless of their stratigraphic position. Thus, the broad trends in Figs. 5 and 6, to a large extent reflect variation in lithologic abundance with stratigraphic position.

Al and Cr contents in spinel (Fig. 8) define the most clearly defined cryptic variations in this study. In general, increasing Al and decreasing Cr in spinel tends to accompany somewhat the more vaguely defined trends of Fe-enrichment in clinopyroxene and olivine. With increasing height in the section, spinel shows a slight enrichment in Al and depletion in Cr in the lower megacrhythm and a major enrichment in Al and depletion in Cr in the upper megacrhythm. In contrast, spinel compositions in transitional zone become more depleted in Al and enriched in Cr with height in the section. Fig. 9 illustrates that the compositional variation of spinel in the lower megacrhythm and the transitional zone are similar. Spinel in the upper megacrhythm overlaps with this field but extends to much more Cr-rich compositions.

COMPARISON TO THE OMAN OPHIOLITE

Taken as a whole, the ranges of mineral compositions in the Voykar layered complex are similar to those reported for the layered gabbro of the Oman Ophiolite in the northern Oman Mountains. Excluding the marginal dunite, which is more magnesian and more properly compared to the uppermost mantle rocks in Oman, the ranges in Mg/(Mg+Fe) for olivine and clinopyroxene of the Voykar layered complex are essentially the same as reported for the layered gabbro of the Rustaq block (Browning, 1984) and the northern Oman Mountains (Smewing, 1981). As in the Voykar massif, gabbro-norite and norite are volumetrically significant in

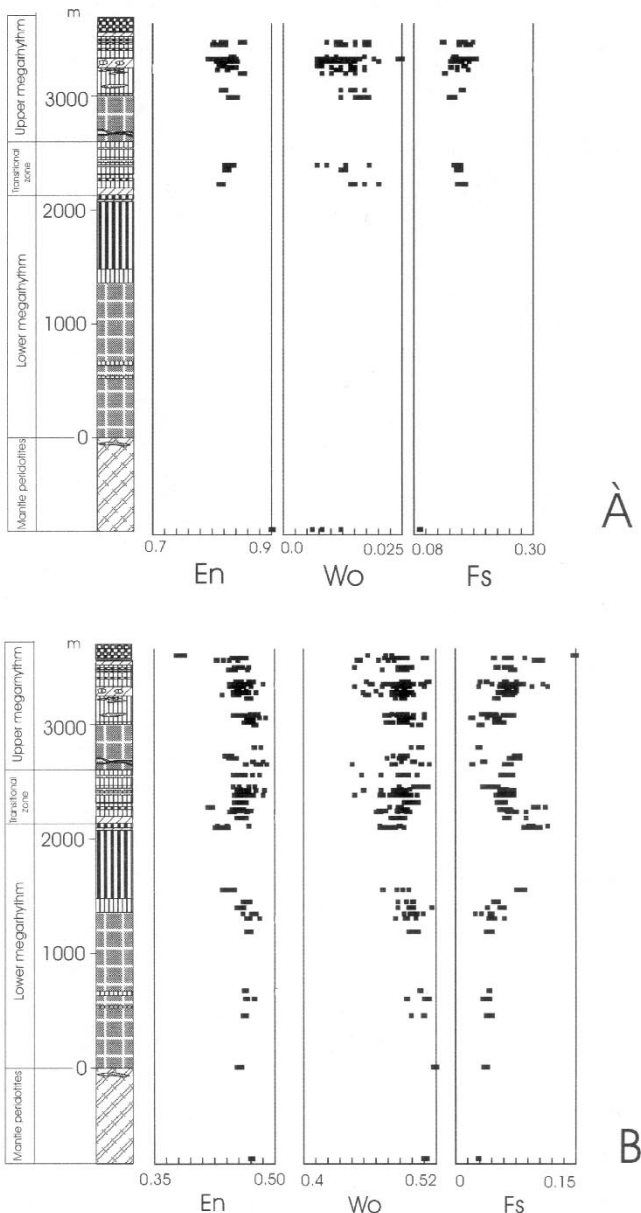


Fig. 6 - Compositional variation of pyroxene through the section. A- orthopyroxene, B- clinopyroxene. Ornamentation as in Fig. 5.

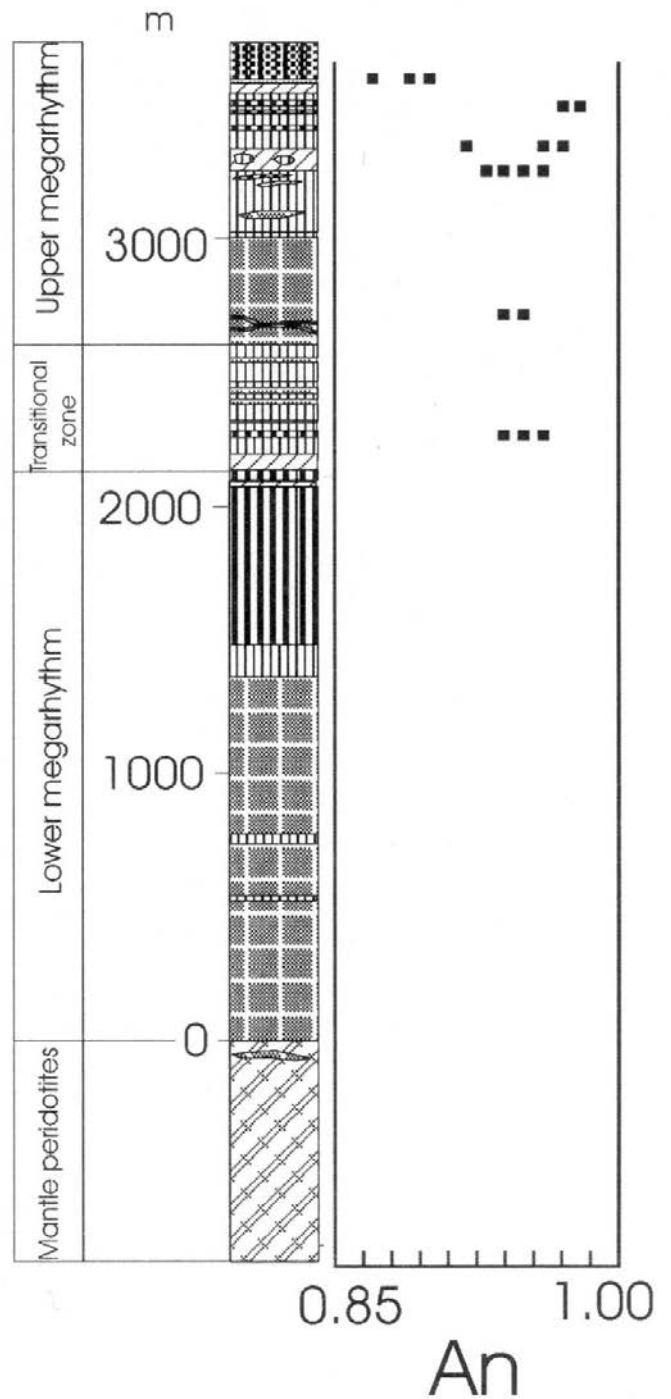


Fig. 7 - Anorthite content of plagioclase through the section. Ornamentation as in Fig. 5.

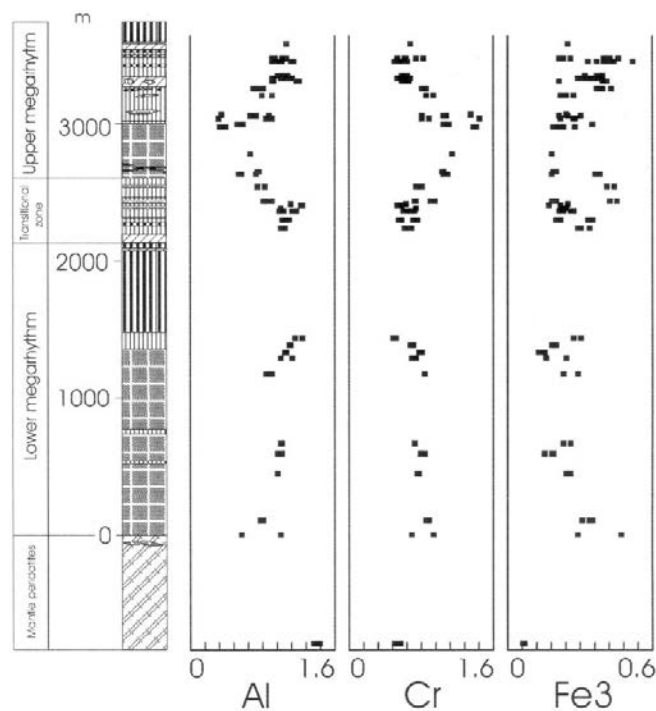


Fig. 8 - Compositional variation of spinel through the section. Ornamentation as in Fig. 5.

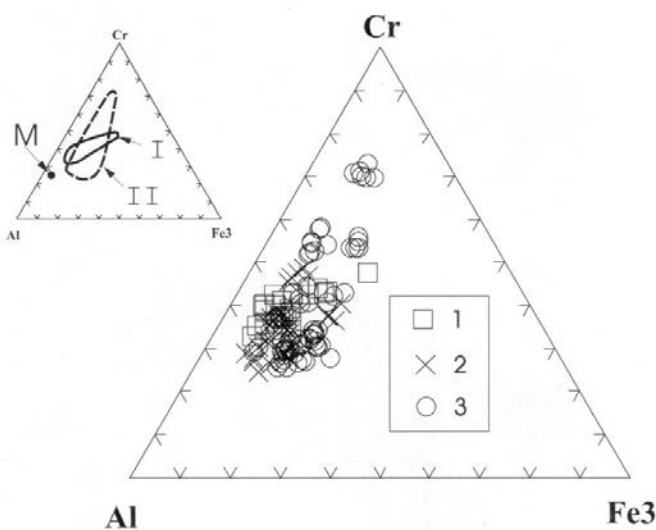


Fig. 9 - Cr-Al-Fe³⁺ compositions of spinel. 1- lower megarhythm; 2- transitional zone; 3- upper megarhythm. In small triangle: fields of spinel from the lower megarhythm (I) and from the upper megarhythm (II); M- mantle spinel from the studied section.

the northern Oman Mountains (Smewing, 1981; Lippard et al., 1986; Juteau et al., 1988). In contrast, more Fe-rich compositions are reported for the layered gabbro of the Ibra area of the southern Oman Mountains (Pallister and Hopson, 1981). Plagioclase compositions in the Voykar layered complex are similar to those in Wadi Ragmi area of the northern Oman Mountains, but they are more anorthitic than plagioclase analyzed elsewhere in the Oman ophiolite, which is generally An^{<90}. The range in Cr/(Cr+Al) ratios in spinels of the Voykar layered complex extend to somewhat lower values than those reported by Pallister and Hopson (1981) for the southern Oman Mountains.

The studied section of the Voykar layered complex, like the layered gabbro of the Oman ophiolite, shows no signifi-

cant closed-system Fe-enrichment trend such as documented in continental layered gabbro complexes such as the Skaergaard (e.g., Wager and Brown, 1967). As described in the Oman ophiolite, the Voykar layered complex contains normal and reverse geochemical gradients defined by Fe/(Fe+Mg) in mafic silicates and Cr/(Cr+Al) in spinel (Figs. 5, 6, 8). In both ophiolites, these normal and reverse gradients are similar in stratigraphic scale and compositional range.

DISCUSSION

Consistent with an ophiolitic origin, the principal characteristics of the Voykar layered complex suggest crystallization from a periodically replenished open magma system in a tectonically dynamic, oceanic environment. The absence of a significant Fe-enrichment through 4 to 5 km of olivine- and pyroxene-rich layered cumulus rock requires an open magma system within which there is an approximate balance between fractional crystallization, eruption, and addition of mantle-derived magma. Laz'ko (1988) concluded that the petrochemical composition of the Voykar ophiolite and its association with island-arc complexes suggest that the Voykar ophiolite most likely consists of fragments of lithosphere formed in a back-arc basin. This conclusion is supported by the presence of the boninite series rocks in the sheeted dyke complex (Simonov et al., 1998). Furthermore, the Sm/Nd isotopic systematics of the Voykar crustal section are compatible with derivation from a MORB source (Sharma et al., 1995), and the mineral compositions and assemblages in the Voykar layered complex are consistent with crystallization from a picobasalt parental melt with tholeiitic affinities (Laz'ko and Sharkov, 1988; Sharkov and Smolkin, 1998). Broad cryptic variation in mineral composition over ≥ 100 m intervals parallel changes in the lithologic abundances and may record changes in the rate of magma supply relative to crystallization and/or tapping of different mantle sources that had been previously depleted to different degrees. The later possibility would be consistent with the study by Sharma et al. (1995), which discovered that some harzburgite samples from the Voykar mantle section have $f^{Sm/Nd}$ and $\epsilon Nd(0)$ that are too high to have been the source for the analyzed samples from the Voykar crustal section. The ubiquitous evidence of high-temperature shearing in the Voykar layered complex is similar to that reported in other ophiolitic layered gabbros (e.g., George, 1978; Girardeau and Nicolas, 1981; Nicolas et al., 1988), and is consistent with deformation at a spreading center whether it be generated by mantle underflow as envisioned by Nicolas et al. (1988) or penetrative flow of a "gabbro glacier" as envisioned by Quick and Denlinger (1992, 1993).

REFERENCES

- Browning P., 1984. Cryptic variation within the cumulate sequence of the Oman ophiolite: Magma chamber depth and petrological implications. In: I.G. Gass et al. (Eds.), *Ophiolites and oceanic lithosphere*, Geol. Soc. London Spec. Publ., 13: 71-82.
- Detrick R.S., 1991. Ridge crest magma chambers: a review from marine seismic experiments at the East Pacific Rise. In: T. Peters, A. Nicolas and R.J. Coleman (Eds.), *Ophiolite genesis and evolution of the oceanic lithosphere*. Kluwer Ac. Publ., Dordrecht/Boston/London, p. 7-20
- Efimov A.A., Lennykh V.I., Puchkov V.N., Saveliev A.A.,

- Savelieva G.N., Jaseva R.G., 1978. Guidebook for excursion "Ophiolites of Polar Urals". Fourth field ophiolite conference, 1-15 August 1978. Moscow, Geol. Inst., USSR Acad. Sci., 165 pp.
- George R.P.J., 1978. Structural petrology of the Olympus Ultramafic Complex in the Troodos ophiolite, Cyprus. *Geol. Soc. Am. Bull.*, 89: 845-865.
- Girardeau J. and Nicolas A., 1981. Structures in two of the Bay of Islands (Newfoundland) ophiolite massifs: A model for oceanic crust and upper mantle. *Tectonophysics*, 77: 1-34.
- Ivanov K.S., 1988. Modern structure of the Urals as a result of the post-Paleozoic extension of the Earth's crust. *Russian Geol. Geophys.*, 39: 204-210.
- Juteau T., Beurrier M., Dahl R. and Nehlig P., 1988. Segmentation at a fossil spreading axis. The plutonic sequence of the Wadi Haymiliayah area (Haylayn Block, Sumail Nappe, Oman). *Tectonophysics*, 151: 167-197
- Laz'ko E.E., 1988. Ultrabasite of ophiolite assemblage. In: E.E.Laz'ko and E.V. Sharkov (Eds.), *Magmatic rocks*, Vol. 5. *Ultramafic Rocks*, Nauka Publ., Moscow, p. 8-96 (in Russian).
- Laz'ko E.E. and Sharkov E.V., (Eds.), 1988. *Magmatic Rocks*. Vol. 5. *Ultramafic rocks*. Nauka Publ., Moscow, 501 pp. (in Russian).
- Lippard S.J., Shelton A.W. and Gass I.G., 1986. The ophiolite of northern Oman. *Mem. Geol. Soc. London*, 11, 178 pp.
- Nicolas A., 1989. *Structures of ophiolites and dynamics of oceanic lithosphere*. Kluwer Academic, Boston, Mass., 367 pp.
- Nicolas A., Reuber I. and Benn K., 1988. A new magma chamber model based on structural studies in the Oman ophiolite. *Tectonophysics*, 151: 87-105
- Pallister J.S. and Hopson C.A., 1981. Samail ophiolite plutonic suite: Field relations, phase variation and layering and a model of a spreading ridge magma chamber. *J. Geophys. Res.*, 86: 2593-2644.
- Puchkov V.N., 1997. Tectonics of the Urals. Present-day views. *Geotectonica*, 4: 42-61.
- Quick J.E. and Denlinger R.P., 1992. The possible role of ductile deformation in the formation of layered gabbros in ophiolites. *Ofioliti*, 17 (2): 249-253.
- Quick J.E. and Denlinger R.P., 1993. Ductile deformation and the origin of layered gabbro in ophiolites. *J. Geophys. Res.*, 98: 14015-14027.
- Saveliev A.A., 1997. Ultramafic-gabbroic associations in the Voykar-Syn'ya ophiolite massif (the Arctic Urals). *Geotectonica*, 1: 48-58.
- Saveliev A.A. and Savelieva G.N., 1979. Ophiolites of the Voykar massif (Polar Urals). In: *Ophiolites of the Canadian Appalachians and Soviet Urals*, Dept. of Geology, Memorial University, Newfoundland, 8: 127-140.
- Savelieva G.N., 1987. Gabbro-ultrabasite assemblages of the Urals ophiolites and their analogues in modern oceanic crust. *Nauka Publ., Moscow*, 245 pp. (in Russian).
- Sharkov E.V., Smolkin V.F., 1998. Palaeoproterozoic layered intrusions of the Russian part of the Fennoscandian Shield: a review. *Trans. Inst. Min. Metallurgy, (Sect.B: Appl. Earth Sci.)*, 107: B23-B38.
- Sharma M., Wasserburg G.J., Papanastassiou D.A., Quick J.E., Sharkov E.V. and Laz'ko E.E., 1995. High $^{143}\text{Nd}/^{144}\text{Nd}$ in extremely depleted mantle rocks. *Earth Planet Sci. Lett.*, 39: 101-114.
- Simonov V.A., Kurenkov S.A. and Stupakov S.I., 1998. Boninite series in the Polar Urals paleospreading complexes. *Dokl. Russian Acad. Sci.*, 361: 232-235.
- Sinton J.M. and Detrick R.S., 1992. Mid-ocean ridge magma chambers. *J. Geophys. Res.*, 97: 197-216.
- Smewing J.D., 1981. Mixing characteristics and compositional differences in mantle-derived melts beneath spreading axes: Evidence from cyclically layered rocks in the ophiolite of North Oman. *J. Geophys. Res.*, 86: 2645-2660.
- Wager L.R. and Brown G.M., 1967. *Layered Igneous Rocks*. W. H. Freeman, San Francisco, 588 pp.
- Zonenshain L.P., Kuz'min M.L. and Natapov L.M., 1990. *Geology of the USSR: A plate tectonic synthesis*. AGU, Washington, D.C., 21, 242 pp.

Received, November 1, 1998

Accepted, October 11, 1999

